Available online at www.sciencedirect.com

ScienceDirect

Procedia Structural Integrity 17 (2019) 624–631

Structural Integrity Procedia

www.elsevier.com/locate/procedia

ICSI 2019 The 3rd International Conference on Structural Integrity

Influence of the SMA constitutive model on the longitudinal seismic response of RC bridges

Pedro Nunes[a], Paulo Silva Lobo[b,a,*]

[a]*Departamento de Engenharia Civil e Geologia, Faculdade de Ciências Exatas e da Engenharia, Universidade da Madeira, Campus Universitário da Penteada, 9000-390, Funchal, Portugal*

[b]*CERIS, Instituto Superior Técnico, Universidade de Lisboa, Av. Rovisco Pais 1, 1049-001, Lisboa, Portugal*

Abstract

Several studies indicate that the re-centring capacity presented by superelastic Shape Memory Alloys (SMA) can reduce the displacements of structures subjected to earthquakes. To quantify the errors of numerical predictions with different constitutive models, peak, relative and residual displacements of four two-framed reinforced concrete (RC) bridges, linked by SMA bars, subjected to seismic actions, were numerically assessed. Different ratios of the elastic natural period of vibration of the frames of the bridges were adopted. Lumped plasticity models were used to simulate the behaviour of the reinforced concrete columns. Five SMA uniaxial models were considered, combining linear, nonlinear, isothermal and nonisothermal conditions. The seismic action was modelled by real accelerograms. The results show that the relative displacements are more sensitive to the adopted SMA model than the peak and residual displacements. Significant relative differences, up to 70%, were obtained.

Peer-review under responsibility of the ICSI 2019 organizers.

Keywords: Shape memory alloys; superelasticity; re-centring; constitutive models; kinetic law; reinforced concrete

1. Introduction

Superelastic Shape Memory Alloys (SMA) can recover from cyclic inelastic axial deformations without significant permanent deformation and possess dissipative properties. These properties led various authors to study the use of SMA for seismic protection of structures. Alam et al. (2012) considered SMA as reinforcement in concrete structures.

* Corresponding author.
E-mail address: plobo@uma.pt

2452-3216
Peer-review under responsibility of the ICSI 2019 organizers.
10.1016/j.prostr.2019.08.084

Andrawes and DesRoches (2005, 2007a, b), Johnson et al. (2008) and Cardone et al. (2011) used SMA restrainers to prevent unseating of reinforced concrete (RC) bridges with joints. McCormick et al (2006) and Silva Lobo et al (2017) evaluated the application of SMA bracing systems in steel frames and RC frames, respectively. Silva Lobo et al. (2015a) and Cismaşiu and Santos (2008) used bridges to study their SMA device proposals.

These authors modelled the axial behaviour of SMA using uniaxial phenomenological models. The latter considered the nonisothermal behaviour of SMA. The remaining used isothermal models, valid only for monotonic loads. Independently from the type of application and model, the results indicate that SMA contribute to the reduction of the displacements during earthquakes and make it possible to re-centre the structure.

It should be noted that studies based on single-degree-of-freedom systems (SDOF) indicate that the SMA model adopted can significantly affect the prediction of displacements. Andrawes and DesRoches (2008) studied the seismic response of linear and nonlinear SDOF with natural periods of vibration T = 0.25, 0.50, 0.75 and 1.0 s using three SMA isothermal models. Nonlinear SDOF were modelled with lumped plasticity models for RC structures. The peak displacement errors obtained for linear and nonlinear SDOF are 9% and 5%, respectively. Bernardini and Rega (2017) conducted a similar study for harmonic loads, using a linear SDOF with T = 0.33 s and six SMA models, three of which are isothermal. Prediction errors as high as 41% were obtained. Andrawes and DesRoches (2007c) studied the effects SMA, using isothermal models and lumped plasticity models for RC, on the seismic response of two coupled nonlinear SDOF with period ratio $T_1/T_2 = 0.7$. Errors less than 10% were obtained for the relative displacements. Nunes and Silva Lobo (2017) conducted a similar study for linear SDOF with $T_1/T_2 = 0.5$, 0.6, 0.7 and 0.8, using four nonisothermal SMA models. Errors up to 16% and 32% were obtained for peak and relative displacements.

The research presented herein extends the latter work for nonlinear SDOF, modelling the longitudinal behaviour of RC bridges. The purpose of this study is to assess the influence of structural ductility on the peak, relative and residual displacements predicted with different SMA models.

2. Case studies and models

The four two-frame RC bridges (C30/37 concrete and A500 NR) studied by Nunes and Silva Lobo (2017) were used as case studies as they make it possible to study peak, relative and residual displacements. The geometry and values of T, mass (m), height (H), elastic stiffness (K_{el}) and yield displacement (u_y) of each frame are shown in Fig. 1. Values of T_1/T_2 equal to 0.5, 0.6, 0.7 and 0.8 were adopted as they cover the range of values expected in real applications. All columns have a cross-section with 2.0 m diameter reinforced with 50ϕ40 longitudinal rebars and ϕ20 hoops spaced at 0.11 m. Its cracked flexural stiffness was determined as being equal to 12551000 kNm^2. This latter value and the values of u_y ($= \phi_y[H+L_{SP}]^2/3$; yield curvature $\phi_y = 0.00275$ m^{-1} and strain penetration length $L_{SP} = 0.968$ m) were determined according to Priestley et al. (2007). K_{el} was obtained assuming the columns with fixed ends.

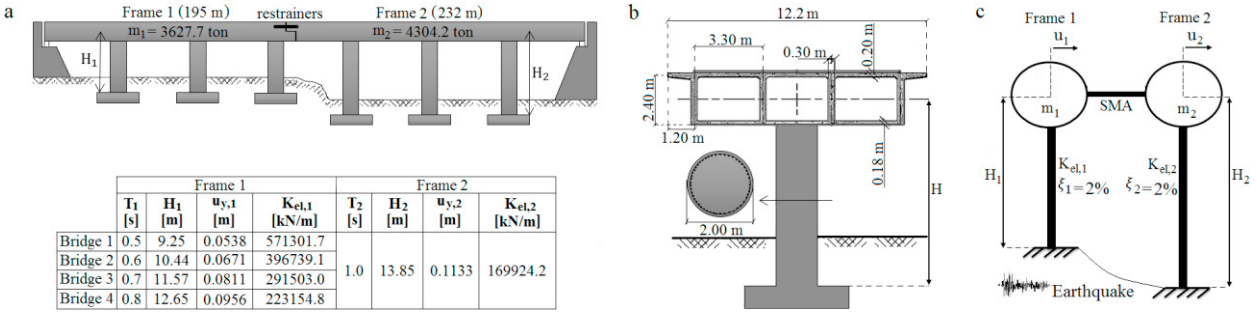

	Frame 1				Frame 2			
	T_1 [s]	H_1 [m]	$u_{y,1}$ [m]	$K_{el,1}$ [kN/m]	T_2 [s]	H_2 [m]	$u_{y,2}$ [m]	$K_{el,2}$ [kN/m]
Bridge 1	0.5	9.25	0.0538	571301.7	1.0	13.85	0.1133	169924.2
Bridge 2	0.6	10.44	0.0671	396739.1				
Bridge 3	0.7	11.57	0.0811	291503.0				
Bridge 4	0.8	12.65	0.0956	223154.8				

Fig. 1 – Bridges used: (a) characteristics and longitudinal profile; (b) superstructure and substructure; (c) scheme of the adopted model

The longitudinal response of the bridges was focused. The analytical models adopted consist of two nonlinear SDOF coupled by SMA bars (see Fig. 1 (c)), representing a retrofit intervention using restrainers to prevent the unseating of the adjacent superstructures (see Fig. 1 (a)). As material non-linearity was modelled, a viscoelastic

damping ratio ξ of 2% was adopted for both SDOF. The soil-structure iteration, pounding between frames and friction at the joint were not modelled. The nonlinear dynamic analysis was performed using a MATLAB programming language-based program based on Newmark's constant average acceleration method (Chopra, 2007).

Nonlinear SDOF were modelled using the modified Clough lumped plasticity model (see Fig. 2). This model accounts for the stiffness degradation of RC structures under cyclic loading as a function of peak displacements, u_{max}, and estimates their residual displacement, u_{res}, as well (Genshu and Yongfeng, 2007). The responses for positive and negative displacements are independent. The effects of strain hardening of reinforcement were modelled using a post-yield stiffness $K_{pl} = 0.05K_{el}$. The degradation of the unloading stiffness was modelled using the equation $K_u = (u_{max}/u_y)^{0.5}$. Muthukumar and DesRoches (2005) also adopted these two options for a similar model. The reloading stiffness K_r is equal to the slope of the line defined by the point of zero force on the unloading branch and u_{max}. If partial unloading occurs, the response point follows the unloading path during reloading.

SMA bars were modelled using five uniaxial models derived from the proposal by Tanaka et al. (1986), named herein as: Linear; Isothermal; Exp_T; Exp_LA3; Exp_LA20. All use the constitutive law by Brinson (1993) to describe the relationship between axial stress, axial strain, martensite fraction and temperature. All except Isothermal use an energy-balance law (Silva Lobo et al., 2015b) to simulate the effect of loading-rate on temperature. The models differ on the kinetic law governing the martensite fraction: Linear and Isothermal use the linear law (Auricchio and Sacco, 1997); Exp_T uses the exponential by Tanaka et al. (1986); Exp_LA3 and Exp_LA20 use two variations of the exponential by Lubliner and Auricchio (1996). The material properties adopted by Cismaşiu and Santos (2008) were used. A comparison of the used models is shown in Fig. 3.

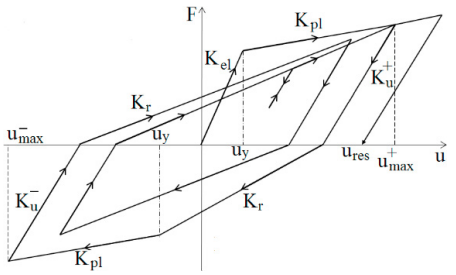

Fig. 2 – Force-displacement relationship of the modified Clough model

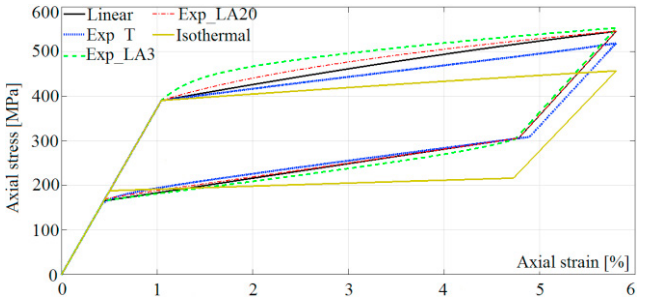

Fig. 3 – Comparison between the SMA models adopted

3. Sensitivity study and discussion of results

The sensitivity study presented herein was performed for an ambient temperature of 20 ºC and six accelerograms (PEER, 2019): Loma Prieta – Corralitos (M = 6.9, PGA = 0.65g, D = 14.0 s); Loma Prieta – Gilroy Array #3 (M = 6.9, PGA = 0.56g, D = 10.0 s); Kobe – Nishi-Akashi (M = 6.9, PGA = 0.48g, D = 16.7 s); San Fernando – Pacoima Dam (M = 6.6; PGA = 0.69g; D = 10.7 s); Northridge – Canonga Park (M = 6.7, PGA = 0.36g, D = 17.9 s); Umbria and Marche – Colfiorito (M = 6.0; PGA = 0.20g; D = 8.9 s). M is the magnitude at moment scale, PGA is the peak ground acceleration, g is the gravitational acceleration and D is the duration. The records were amplified using factors AF = 2.0 and 3.0 to explore the effects of the ductility of the structure. The peak displacements of the SDOF 1 and 2, $u_{1,max}$ and $u_{2,max}$, the related residual displacements, $u_{1,res}$ and $u_{2,res}$, the peak relative displacement, $\Delta_{u,max}$, and the relative residual displacement, $\Delta_{u,res}$, were focused (see Fig. 4).

SMA bars were designed based on $\Delta_{u,max}$ obtained in the analysis of the uncoupled SDOF (see Fig. 5). A target displacement, $\Delta_{u,T}$, equal to one-third of $\Delta_{u,max}$, and a SMA target strain of 6% were adopted as design parameters for each AF. The cross-sectional area A_{SMA} was determined iteratively for all T_1/T_2 and AF. This design was performed using the Corralitos record, because it is one of the most demanding records used, and the Linear model. For simplicity, the SMA length (L_{SMA}) was determined for the largest $\Delta_{u,T}$ of each AF. The results obtained are shown in Table. 1. As expected, the values of A_{SMA} and L_{SMA} increased with the increase of AF and decreased with the increase of T_1/T_2.

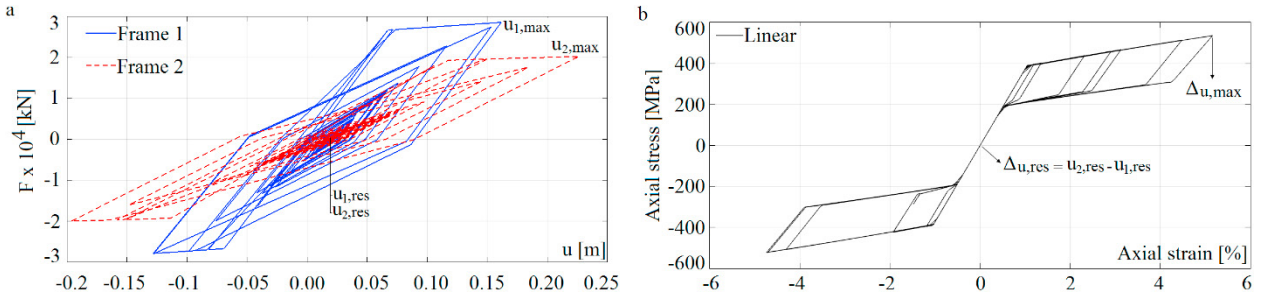

Fig. 4 – Behaviour of RC SDOF (a) and SMA (b) for a particular analysis (Colfiorito record, with AF = 3.0 and $T_1/T_2 = 0.6$)

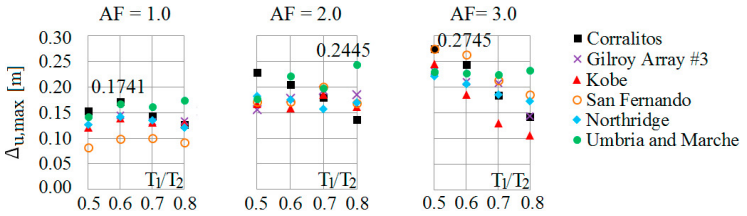

Fig. 5 – Values of $\Delta_{u,max}$ obtained in the seismic analysis of the uncoupled SDOF (peak values indicated in each figure)

Table. 1. Values of A_{SMA} and L_{SMA} determined for each AF and T_1/T_2

AF	A_{SMA} [cm^2] $T_1/T_2 = 0.5$	A_{SMA} [cm^2] $T_1/T_2 = 0.6$	A_{SMA} [cm^2] $T_1/T_2 = 0.7$	A_{SMA} [cm^2] $T_1/T_2 = 0.8$	$\Delta_{u,M}$ [m]	$\Delta_{u,T}$ [m]	L_{SMA} [m]
1.0	285.9	204.9	140.3	81.1	0.1741	0.0580	0.967
2.0	291.7	211.3	148.9	97.6	0.2445	0.0815	1.358
3.0	329.7	222.5	152.5	99.9	0.2745	0.0915	1.526

3.1. Peak and residual displacements

The values of $u_{1,max}$ and $u_{2,max}$ obtained with the Linear model are presented in the first column of Fig. 6 (a) and (b). As can be seen, both parameters change with T_1/T_2 and seismic record. Furthermore, most obtained values increased with the increase of AF, as could be expected, allowing the use of the structural ductility (the points above the line u_y indicate that the frames yielded). In the other columns these values are compared with those obtained with other models, using absolute relative differences RD = |[u(Linear) – u(Other)] / u(Linear)|×100. The peak RD are indicated in each figure. This methodology was adopted for relative and residual displacements as well.

For $u_{1,max}$, RD less than or equal to 10% were obtained in 92%, 91% and 88% of the analyses performed for AF = 1.0, 2.0 and 3.0, respectively. For $u_{2,max}$, those values were of 99%, 99% and 98%. These results indicate that the peak displacements are less sensitive to the characteristics of the SMA model, sensitivity which seems to decrease with the increase of the flexibility of the structure. However, the peak RD obtained using each model indicate that exceptions may occur. For $u_{1,max}$ and $u_{2,max}$, it can be seen that peak RD are concentrated in the interval $0.5 \leq T_1/T_2 \leq 0.7$. More specifically, for $u_{1,max}$ and AF = 1.0, 2.0 and 3.0, the obtained peak RD were 26%, 32% and 33%. For $u_{2,max}$, those values decreased to 11%, 15% and 13%. The mentioned values were all obtained with the Exp LA3, which is a model that results in a force greater than the one resulting from the Linear model (see Fig. 3). Even with Exp LA20, which is similar to the Linear model, a peak RD of 14% was obtained for $u_{1,max}$. With the Exp T and Isothermal models, peak RD of 22% and 18% were obtained, also for $u_{1,max}$. For $u_{2,max}$, the peak RD obtained with models other than Exp_LA3 were less than 10%, resulting from one analysis performed with the Isothermal model, AF = 1.0 and $T_1/T_2 = 0.5$.

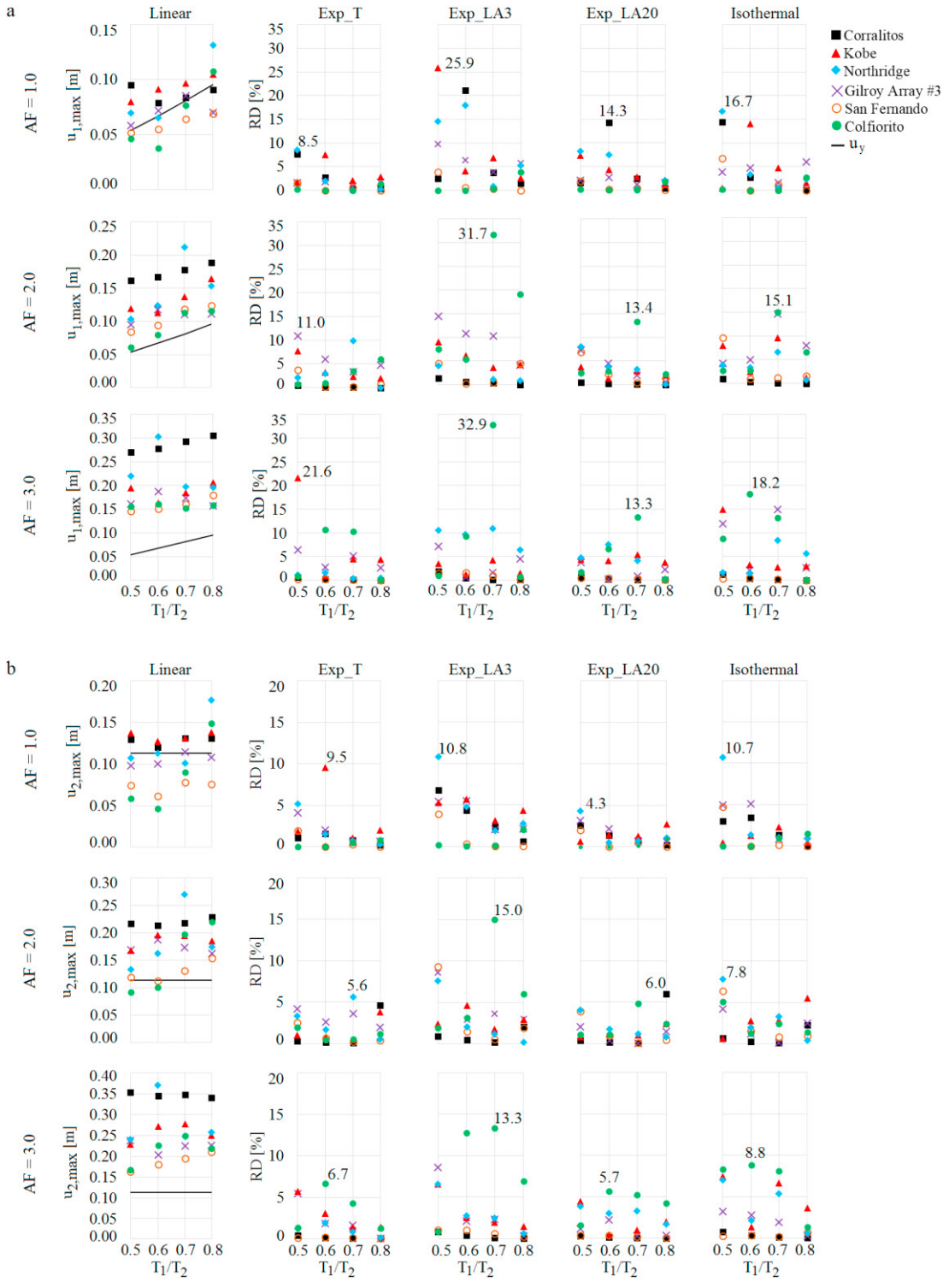

Fig. 6 – Influence of different SMA models on the values of: (a) $u_{1,max}$; (b) $u_{2,max}$

As shown in Fig. 7, there is no correlation between the values of RD obtained for $u_{1,max}$ and $u_{2,max}$, and the ductility ratio $u = u_y/u_{max}$. The peak RD of 15% concerning $u_{2,max}$ was obtained for a peak u of 1.5, which is less than the peak u of 2.5 for which the peak RD of 33%, concerning $u_{1,max}$, was obtained. Both values were obtained for $T_1/T_2 = 0.7$. Despite the evidences, the largest RD obtained for values of u greater than or equal to 3 was of 11%. This indicates that the peak displacements are less sensitive to the SMA model adopted when the structure dissipates more energy. The results also suggest that the model adopted is less relevant for highest T_1/T_2.

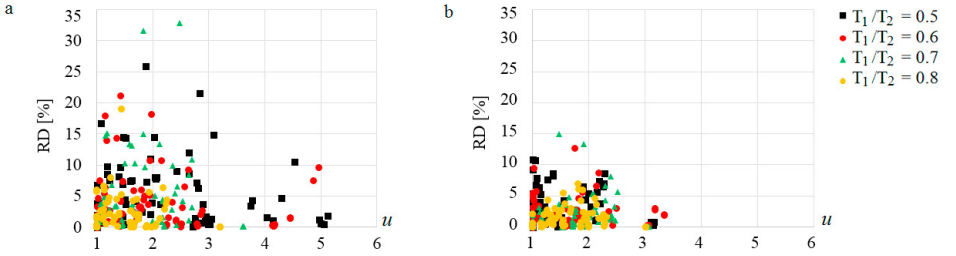

Fig. 7 – Influence of the ductility ratio on the values of RD obtained for: (a) $u_{1,max}$; (b) $u_{2,max}$

Virtually null $\Delta_{u,res}$ were obtained with all SMA models in the analyses performed. Thus, no comparison was made regarding this parameter. As $\Delta_{u,res} = u_{1,res} - u_{2,res}$, the study focused on $u_{2,res}$. The values obtained with the Linear model are presented in Fig. 8. Likewise $u_{1,max}$ and $u_{2,max}$, $u_{2,res}$ was affected by T_1/T_2 and seismic record used, and tended to increase with the increase of AF. The maximum value of 0.12 m was obtained for AF = 3.0, with $T_1/T_2 = 0.6$.

The comparison of different models for a particular analysis was performed only when at least one of the values of $u_{2,res}$ obtained with one of the models was higher than or equal to 0.025 m. This criterion was used to eliminate large RD resulting from the comparison of values of $u_{2,res}$ with small magnitudes. The RD obtained are depicted in Fig. 9. As can be seen, most values are less than 20%. The peak RD is 32%.

As can be seen in Fig. 10, there is no correlation between the values of RD obtained and the ductility ratio of frame 2. The 32% peak RD was obtained for $T_1/T_2 = 0.5$ and $u = 2$.

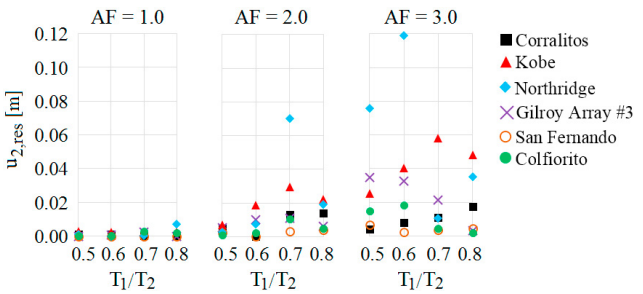

Fig. 8 – Values of $u_{2,res}$ obtained with the Linear model

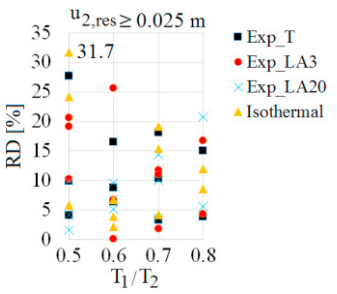

Fig. 9 - Influence of different SMA models on $u_{2,res}$

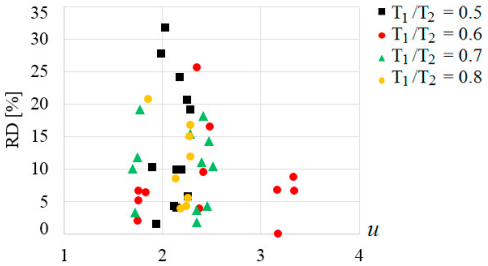

Fig. 10 – Influence of the ductility ratio of frame 2 on the values of RD concerning $u_{2,res}$

3.2. Relative displacements

In Fig. 11, the results regarding $\Delta_{u,max}$ are presented. Like the other parameters studied, $\Delta_{u,max}$ varied with T_1/T_2 and seismic record used and tended to increase with the increase of AF. The peak RD obtained for AF = 1.0 is 76% and was obtained with the Isothermal model for T_1/T_2 = 0.6. For AF = 2.0 and 3.0, peak RD of 72% and 70% were obtained, both when the Exp_LA3 model was used. With the Exp_T model, peak RD of 62% and 40% were obtained for AF = 2.0 and 3.0. These four values were obtained for T_1/T_2 = 0.7. In global terms, values of RD less than or equal to 10% were obtained in 46% of the analyses, independently of the model used. These results indicate that $\Delta_{u,max}$ is more sensitive to the characteristics of the SMA models than all other parameters focused.

As can be seen in Fig. 12 (a) and (b), there is no correlation between the obtained RD and the values of *u* of frames 1 and 2. The maximum RD of 76% was obtained for T_1/T_2 = 0.6 when both frames exhibited values of *u* close to 1. For all T_1/T_2, RD greater than 50% were obtained, what confirms that T_1/T_2 may affect $\Delta_{u,max}$. The values of RD obtained tended to decrease with the increase of *u*, result also observed for the other parameters focused.

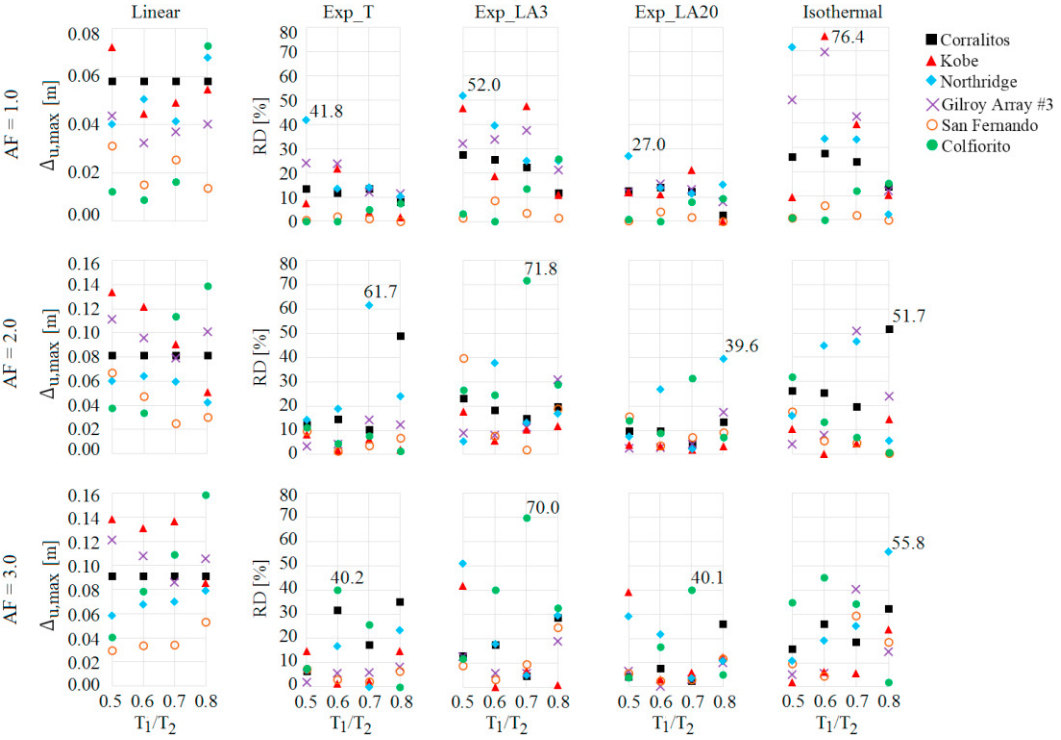

Fig. 11 – Influence of different SMA models on the values of $\Delta_{u,max}$

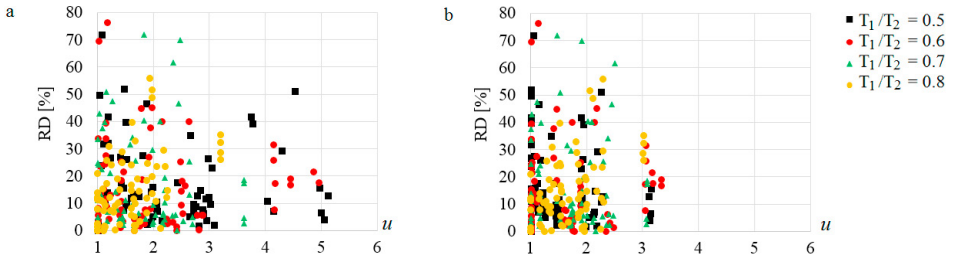

Fig. 12 – Sensitivity of the values of RD concerning $\Delta_{u,max}$ to the ductility ratio of: (a) frame 1; (b) frame 2

4. Conclusions

The seismic response of nonlinear single-degree-of-freedom systems (SDOF) with natural period ratios of 0.5, 0.6, 0.7 and 0.8 coupled by SMA bars was studied using five different SMA uniaxial models. The displacements obtained with those models were compared using relative differences (RD). Major RD of 33% and 32% were obtained for the SDOF peak and residual displacements. Regarding the relative displacements, values of RD as high as 77% were obtained. Furthermore, negligible relative residual displacements were obtained with all SMA models. In global terms, the results obtained indicate that the SMA model adopted may significantly affect predictions of the displacements of structures subjected to earthquakes. The values of RD obtained for each type of displacement were related with the ductility ratio. Even though no evident correlation was found, a tendency of RD decreasing with the increase of the ductility ratio was observed. This indicates that the differences of the SMA models lose relevance with the increase of the plastic incursions of the analyzed structures.

References

Alam, M.S., Moni, S., Tesfamariam, S., 2012. Seismic overstrength and ductility of concrete buildings reinforced with superelastic shape memory alloy rebar. Engineering Structures 35, 8-20.

Andrawes, B., DesRoches, R., 2005. Unseating Prevention for Multiple Frame Bridges Using Superelastic Devices. Smart Materials and Structures 14(3), S60–S67.

Andrawes, B., DesRoches, R., 2007a. Comparison Between Shape Memory Alloy Seismic Restrainers and Other Bridge Retrofit Devices. Journal of Bridge Engineering 12 (6), 700–709.

Andrawes, B., DesRoches, R., 2007b. Effect of Ambient Temperature on the Hinge Opening in Bridges with Shape Memory Alloy Seismic Restrainers. Engineering Structures 29(9), 2294–2301.

Andrawes, B., DesRoches, R., 2007c. Effect of Hysteretic Properties of Superelastic Shape Memory Alloys on the Seismic Performance of Structures. Structural Control and Health Monitoring 14(2), 301–320.

Andrawes, B., DesRoches, R., 2008. Sensitivity of Seismic Applications to Different Shape Memory Alloy Models. Journal of Engineering Mechanics 134(2), 173–183.

Auricchio, F., Sacco, E., 1997. A One-Dimensional Model for Superelastic Shape-Memory Alloys with Different Elastic Properties Between Austenite and Martensite. International Journal of Non-Linear Mechanics 32(6), 1101–1114.

Bernardini, D., Rega, G., 2017. Evaluation of different SMA models performances in the nonlinear dynamics of pseudoelastic oscillators via a comprehensive modelling framework. International Journal of Mechanical Sciences 130, 458-475.

Brinson, L. C., 1993. One-Dimensional Constitutive \ of Shape Memory Alloys: Thermomechanical Derivation with Non-Constant Material Functions and Redefined Martensite Internal Variable. Journal of Intelligent Material Systems and Structures 4(2), 229–242.

Cardone, D., Perrone, G., Sofia, S., 2011. Numerical Studies on the Seismic Retrofit of Bridges Using Shape Memory Alloys. Journal of Materials Engineering and Performance 20(4-5), 535–543.

Cismaşiu, C., Santos, F., 2008. Numerical Simulation of Superelastic Shape Memory Alloys Subjected to Dynamic Loads. Smart Materials and Structures 17(2), 25–36.

Chopra, A.K., 2007. Dynamics of Structures: Theory and Applications to Earthquake Engineering, Third Edition.

Genshu, T., Yongfeng, Z., 2007. Seismic force modification factors for modified-Clough hysteretic model. Engineering Structures 29, 3053-3070.

Johnson, R., Padgett, J. E., Maragakis, M. E., DesRoches, R., Saiidi, M.S., 2008. Large Scale Testing of Nitinol Shape Memory Alloy Devices for Retrofitting of Bridges. Smart Materials and Structures 17(3), pp. 10.

Lubliner, J., Auricchio, F., 1996. Generalized Plasticity and Shape-Memory Alloys. International Journal of Solids and Structures 33(7), 991–1003.

McCormick, J., DesRoches, R., Fugazza, D., Auricchio, F., 2006. Seismic Vibration Control Using Superelastic Shape Memory Alloys. Journal of Engineering Materials and Technology 128(3), 294–301.

Muthukumar, S., DesRoches, R., 2005. Effect of Frame-Restoring Force Characteristics on the Pounding Response of Multiple-Frame Bridges. Earthquake Spectra 21(4), 1113-1135.

Nunes, P., Silva Lobo P., 2017. Influence of the SMA Constitutive Model on the Response of Structures. Procedia Structural Integrity 5, 187-194.

PEER., 2019. http://ngawest2.berkeley.edu/site.

Priestley, M. J. N., Calvi, G. M., Kowalsky, M. J., 2007. Displacement-Based Seismic Design of Structures. IUSS Press, Pavia, Italy.

Silva Lobo, P., Almeida, J., Guerreiro, L., 2015a. Semi-Active Device Based on Superelastic Shape Memory Alloys. Structures 3, 1-12.

Silva Lobo, P., Almeida, J., Guerreiro, L., 2015b. Shape Memory Alloys Behaviour: A Review. Procedia Engineering 114, 776–783.

Silva Lobo, P., Almeida, J., Guerreiro, L., 2017. Recentring and control of peak displacements of a RC frame using damping devices. Soil Dynamics and Earthquake Engineering 94, 66-74.

Tanaka, K., Kobayashi, S., Sato, Y., 1986. Thermomechanics of Transformation Pseudoelasticity and Shape Memory Effect in Alloys. International Journal of Plasticity 2(1), 59–72.